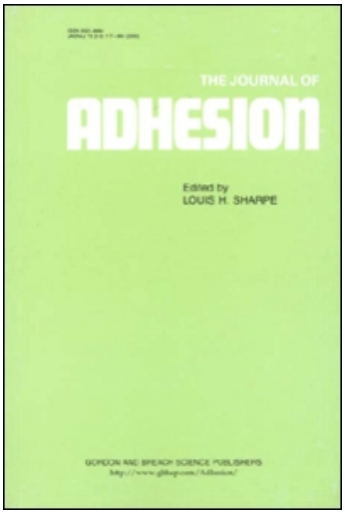

The Journal of Adhesion

Publication details, including instructions for authors and subscription information:
http://www.informaworld.com/smpp/title~content=t713453635

Templating Surfaces with Gradient Assemblies

Jan Genzer[a]
[a] Department of Chemical & Biomolecular Engineering, North Carolina State University, Raleigh, North Carolina, USA

To cite this Article Genzer, Jan(2005) 'Templating Surfaces with Gradient Assemblies', The Journal of Adhesion, 81: 3, 417 — 435
To link to this Article: DOI: 10.1080/00218460590944855
URL: http://dx.doi.org/10.1080/00218460590944855

The Journal of Adhesion, 81:417–435, 2005

ISSN: 0021-8464 print/1545-5823 online
DOI: 10.1080/00218460590944855

Taylor & Francis
Taylor & Francis Group

Templating Surfaces with Gradient Assemblies*

Jan Genzer
Department of Chemical & Biomolecular Engineering, North Carolina State University, Raleigh, North Carolina, USA

*One of the most versatile and widely used methods of forming surfaces with position-dependent wettability is that conceived by Chaudhury and Whitesides more than a decade ago [*Science ***256***, 1539 (1992)]. In this paper we review several projects that utilize this gradient-forming methodology for: controlled of deposition of self-assembled monolayers on surfaces, generating arrays of nanoparticles with number density gradients, probing the mushroom-to-brush transition in surface-anchored polymers, and controlling the speed of moving liquid droplets on surfaces.*

Keywords: Molecular gradient; Self-assembly; Directed assembly

Received 3 September 2004; in final form 7 February 2005.

*This paper is dedicated to Professor Manoj K. Chaudhury for his contributions to the field of self-assembly and surface chemistry. The author is grateful for countless fruitful discussions he has had with Professor Chaudhury over the past several years, his friendship, encouragement, and overwhelming support. The author wants to acknowledge all past and current post-doctoral and doctoral students from his group who have contributed to the various projects outlined in this paper: Dr. Kirill Efimenko, Dr. Tao Wu, Rajendra R. Bhat, Michael R. Tomlinson, Tiffani N. Bailey, and Randal J. Petrie. The author also thanks Dr. Daniel A. Fischer (NIST) and Professor Christopher S. Gorman (NCSU) for their collaboration during the various stages of the research described in this paper. We are grateful to the National Science Foundation, The Camille & Henry Dreyfus Foundation, and 3M for their generous financial support. NEXAFS spectroscopy experiments were carried out at the National Synchrotron Light Source, Brookhaven National Laboratory, which is supported by the U. S. Department of Energy, Division of Materials Sciences and Division of Chemical Sciences.

Address correspondence to Jan Genzer, Department of Chemical and Biomolecular Engineering, North Carolina State University, Raleigh, NC 27695-7905. E-mail: jan_genzer@ncsu.edu

INTRODUCTION

Tuning the surface characteristics of materials, including lubrication or wetting, has become of paramount interest in many everyday applications. While in some situations materials are required to be completely wettable, such as the surfaces of metals before paint deposition, in other applications one needs to prevent the surfaces from being wetted. Examples of the latter include non-stick layers, marine anti-fouling coatings, surfaces of car windshields or frying pans. Altering the surface properties of materials can be achieved by either destructive or constructive means [1]. The first class of methodologies involves techniques such as plasma or corona treatment, or chemical etching. While these methods are widely adopted in various industries, mainly because of their ease of use and scaleability, one typically does not attain a complete molecular-level control over the nature and distribution of the surface functional groups. The second class of technologies involves controlled deposition of self-assembled monolayers (SAMs), Langmuir-Blodgett (LB) films, or polymers [2, 3]. Typically, one employs these methods to achieve much better control over the physico-chemical characteristics of surfaces, albeit on a small scale. For example, the surface of silica or gold can be decorated with SAMs made of organosilane- or thiol-based molecules, respectively. The properties of the newly formed surfaces are then defined by the intimate interplay between the chemical character of the modifying molecules (more specifically, their end-functionality) and their density on the surface.

Over the past several years, much effort has been dedicated to developing methods of generating surfaces with spatially dependent surface chemistries. In particular, recent advances in the field of self-assembly and functionalization have led to the development of a plethora of new technologies based on soft lithography [4], which enable alternative ways of fabricating two- and three-dimensional patterns on material surfaces. Most of the soft lithography techniques are based on controlled deposition of SAMs [2]. Various structural patterns with dimensions ranging from hundreds of nanometers to several micrometers are created on the material surface using a "pattern-transfer element" or stamp that has a three-dimensional structure molded onto its surface. Because of the molecular nature of the SAMs, the surface patterns generated via "soft lithography" are rather thin (several Angstroms to several nanometers). Some applications, particularly those involving subsequent microfabrication steps, such as etching, require that thicker layers of the surface coating be formed. Hence techniques, involving the patterning of thicker

polymer layers grafted to the substrate have been developed [5]. The latter group of technologies is based on selectively decorating the material surfaces with polymerization initiators and then performing the polymerization directly on the surface ("grafting from"). Using this technology, the thickness of the overcoat film can be adjusted by simply varying the polymerization conditions (time, monomer concentration, temperature).

While useful for creating substrates with well-defined chemical patterns of various shapes and dimensions, the soft-lithography technologies always produce sharp boundaries between the distinct chemical regions on the substrate. However, for some applications, it is desirable that the physico-chemical characteristics, such as wetting of the substrate, change gradually. This can be accomplished by producing surfaces with a position-dependent and gradually varying chemistry. In these so-called "gradient surfaces," the gradient in surface energy is responsible for a position-bound variation in surface physical properties, most notably the wettability [6]. We have recently reviewed the various methods leading to the formation of molecular gradients [7, 8]. Covering length scales ranging from nanometers to centimeters, these methodologies offer the prospect of meeting the demands of a variety of novel applications. For example, such gradient substrates can useful in high-throughput studies of the interfacial behavior of molecules and macromolecules [9] (the entire behavioral spectrum can be accessed in a single experiment), they can serve as templates for further processing [9], or be used as active elements in controlled surface transport of materials [10].

Over the past four decades, multiple methods have been conceived and developed that facilitated fabrication of such gradient substrates [6, 7]. The first report describing formation of wettability gradients dates back to the mid 1960s to the work of Carter, who described a technique based on evaporating palladium metal on cellulose acetate-covered glass [11]. In the mid 1980s, Elwing proposed a new method of preparing molecular gradients [12]. In his technique, the wettability gradient on the solid silicon-oxide covered substrate was produced by diffusion of dichlorodimethyl silane (DDS) between two mutually soluble organic solvents with different densities. In a typical experiment, a silica-covered substrate was placed vertically into a container that was filled with xylene. Trichloroethylene (TCE) was mixed with a small amount of DDS and was delivered under the xylene phase in the container. During the incubation the two solvents interdiffused, the DDS diffused to the xylene region and was simultaneously attached to the silica surface. While relatively simple, the technique has severe limitations, which included rather complicated set up,

strict requirements on the solubility of the solute, etc. More than a decade ago, Chaudhury and Whitesides proposed a relatively simple modification to the Elwing's method [13]. Namely, rather than utilizing the liquid phase as a carrier for the depositing molecules, the suggested delivering the gradient-forming molecule through the vapor. In their technique, the diffusing source, comprising a mixture of high vapor pressure organosilane and paraffin oil (PO), was placed on one side of the silica-covered substrate; the whole system was placed into a closed container. The concentration of the diffusing source was conveniently adjusted by simply varying the organosilane: PO ratio. As the silane evaporated, it diffused in the vapor phase and generated a concentration gradient along the substrate. Upon impinging on the substrate, the organosilane molecules reacted with the substrate—OH functionalities on the substrate and formed a wettability gradient. Using this set up, Chaudhury and Whitesides demonstrated the ability of gradient substrates to set liquids in motion (they moved a water droplet uphill) and established the effect of the contact angle hysteresis on the droplet transport. While seemingly minor, Chaudhury and Whitesides's suggestion to replace the liquid for vapor not only removed the aforementioned limitations of the Elwing's method but also allowed for further fine-tuning of the gradient properties. The robustness and versatility of the vapor deposition methodology has inspired us to utilize it in our research.

Our group has used the aforementioned vapor deposition gradient method in different modifications in several research projects. In this paper we highlight a few examples, including: molecular aspects of deposition of self-assembled monolayers on surfaces, generating two-dimensional arrays of nanoparticles, probing the mushroom-to-brush transition in surface-anchored polymers, and controlling the speed of moving liquid droplets on surfaces.

MOLECULAR STRUCTURE OF SELF-ASSEMBLED MONOLAYERS

One of the most important properties of a molecular gradient is its wettability, which is determined primarily by the chemical nature of the terminal group of the SAM and the concentration of molecules attached to the substrate at a given position along the gradient. Various types of gradient geometries can be generated, which involve single directional gradients, double directional gradients (in either opposite or orthogonal directions), or radial gradients. The gradual variation of the grafting density of the surface-bound molecules is expected to have profound influence on the organization of the

molecules in the gradients. By studying how the gradient-forming molecules arrange across the gradient interfacial region one can learn more about the mechanisms and nature of self-assembly in organosilane SAMs. The gradient geometry offers the advantage of constraining the self-assembly growth into a given direction. This is in contrast to the classical case of self-assembly on a homogeneous substrate, where the incorporation of the molecules in the final SAM takes place at random in all directions.

Our group has been actively studying the organization of molecules in the SAMs using various techniques, in particular using synchrotron-based near-edge X-ray absorption fine structure (NEXAFS) spectroscopy. NEXAFS involves the resonant soft X-ray excitation of a K or L shell electron to an unoccupied low-lying antibonding molecular orbital of σ or π symmetry, σ^* and π^*, respectively [14]. The initial state K or L shell excitation gives NEXAFS its element specificity, while the final-state unoccupied molecular orbitals provide NEXAFS with its bonding or chemical selectivity. A measurement of the intensity of NEXAFS spectral features enables the identification of chemical bonds, determination of their relative population density and orientation within the sample.

The ability of NEXAFS to determine the molecular orientation of the surface-bound molecules can be utilized to study the orientation of the SAMs across the gradient. [15, 16]. Most of our work concentrated on the organization of 1H,1H,2H,2H-Perfluorodecyl organosilanes ($F(CF_2)_8(CH_2)_2-Si\equiv$, F8H2) in the SAMs. In Figure 1 we plot the dependence of fraction of F8H2 on the surface (normalized by the maximum SAM coverage) (solid lines) and the variation of the average tilt of the semifluorinated part of the F8H2 molecule with respect to the surface normal, $\langle\tau_{F8}\rangle$, (dashed lines) as a function of the position on the silica surface for mono- ($F8H2-(CH_3)_2Cl$, m-F8H2), di- ($F8H2-(CH_3)Cl_2$, d-F8H2), and tri-functional ($F8H2-Cl_3$, t-F8H2) moieties [17]. By comparing the information about the concentration and orientation of F8H2 in the molecular gradient the following picture emerges. Close to the diffusing sources, the density of the F8H2 molecules is high and as a result complete SAMs form, similar to homogeneous F8H2 SAMs [15, 18]. At larger distances from the diffusing sources, the concentration of F8H2 molecules decreases. Interestingly, the functional dependence of the concentration profiles varies, depending on the type of bonding on the substrate. This can be due to several factors. First, with the exception of the monofunctional m-F8H2 molecules, both d-F8H2 and t-F8H2 species have a tendency to assemble into larger multimolecular clusters. This behavior has been known for some time and is relatively well documented [19].

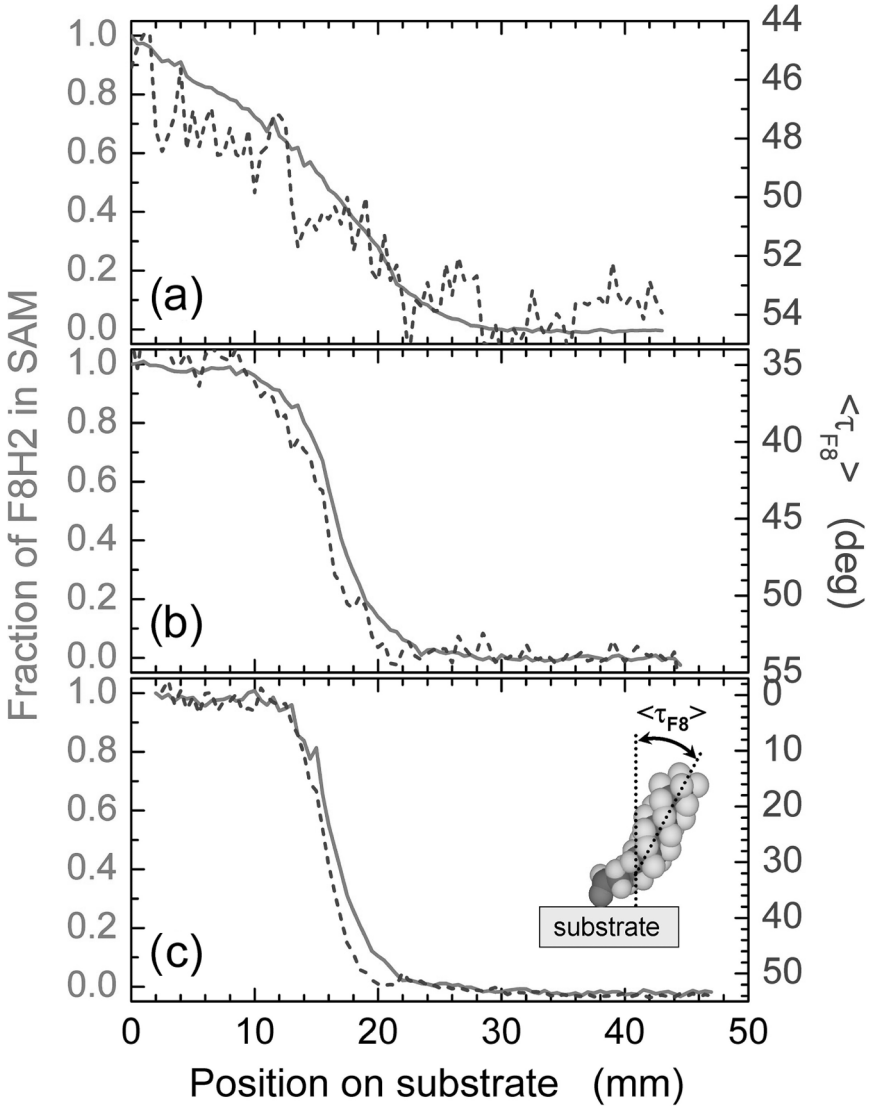

FIGURE 1 Fraction (solid lines) and the molecular orientation (dashed lines) of F8H2 in the molecular gradients made of m-F8H2 (a), d-F8H2 (b), and t-F8H2 (c) organosilanes as a function of the position on the substrate. The inset to the figure shows a schematic of the molecular orientation of a single F8H2 molecule in t-F8H2 SAM and denotes the definition of $\langle \tau_{F8} \rangle$. [Reprinted from reference 8, with permission from American Scientific Publishers.]

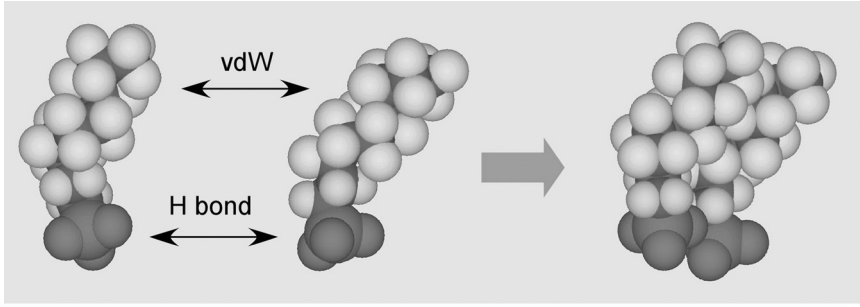

FIGURE 2 Schematic representing the formation of 1H,1H,2H,2H-Perfluorodecyl trihydroxy silane complexes (hydrolyzed version of t-F8H2). Both strong van der Waals forces acting among the $-(CF_2)-$ helices and hydrogen bonds between hydroxyls on the neighboring chains are responsible for the formation of t-F8H2 clusters.

These clusters can form either in the vapor phase or/and after the molecules hit the silica surface. Recall that only minute concentrations of water are needed to hydrolyze the Si−Cl bond, thus converting it into Si−OH. The cluster formation is facilitated by either hydrogen bonds acting between the hydroxyls from several molecules or by forming Si−O−Si linkages via condensation between neighboring Si−OH groups. Moreover, the long-living nature of such clusters is further facilitated by rather strong intermolecular van der Waals forces acting between two or more $-(CF_2)_8-$ helices (Fig. 2). Thus unlike the m-F8H2 SAMs, that are formed primarily by deposition of single molecules, the d-F8H2 and t-F8H2 SAMs may be built by inserting clusters containing multiple molecules. The second factor, which is closely associated with the first one, has to do with the way the F8H2 organosilanes pack. We have recently reported that the orientation of the F8H2 molecules in homogeneous SAMs depends on the bonding environment of the F8H2 molecule. The average tilt angles of the semifluorinated part of t-F8H2, d-H8H2, and m-F8H2 moieties form the surface normal, $\langle \tau_{F8} \rangle$, were $10 \pm 2^\circ$, $35 \pm 2^\circ$, and $45 \pm 3^\circ$, respectively [20]. The increase of the tilt angle with increasing number of the methyl groups attached to the silicon terminus was associated with the steric hindrance of those methyl groups close to the bonding substrate. From Figure 1, $\langle \tau_{F8} \rangle$ increases as one moves away from the diffusing source along each gradient. This behavior suggests that the chains start deviating from their tilts in the homogeneous SAMs. This molecular reorganization of the F8H2 molecules is in part due to the decreasing grafting density on the surface. Considering that the spot

size of the X-ray beam on the sample during the NEXAFS experiments, $\approx 1\,mm^2$, is much larger than the area occupied by a single t-F8H2 molecule, the tilt angle $\langle \tau_{F8} \rangle$ determined from NEXAFS represents only an *average* value. Hence, there is no straightforward way to discriminate between the case of all t-F8H2 molecules homogeneously tilting by the same angle and the case of a disordered system with a broad distribution of tilt angles. Therefore the increase in $\langle \tau_{F8} \rangle$ observed in the region of the gradient in which the concentration decreases cannot be unambiguously interpreted by using the NEXAFS data alone. Complementary measurement of another physical property along the gradient—such as the density and/or the thickness—is required [21].

We note that the description of the mechanism involved in the formation of molecular gradients was rather vague. In their original paper [13], Chaudhury and Whitesides postulated that the gradient parameters, including gradient steepness and molecular concentration, depend primarily on the molecular diffusion in the vapor phase, which is influenced by the vapor pressure of the diffusing species and the concentration of the organosilane moieties in the diffusing source. Ongoing work in our group indicates that the gradient-forming mechanism is much more complex. Specifically, in addition to the two aforementioned properties, the gradient properties also depend on the geometry of the diffusing system (confined vs. unconfined), and the condition of the vapor phase (relative humidity, nature of gas). In addition to the vapor diffusion, surface mobility is also important in determining the organization of the molecules in the gradient SAMs. This is influenced by the concentration of the "sticky" groups on the surface and those on the molecule. The latter will vary with the end-functionality of the organosilane (m- *vs*. d- *vs*. t-) and will depend on whether the molecules are incorporated into the gradient as individual moieties or as clusters. Work is currently in progress to address the influence of these phenomena [21].

The main limitation of the vapor diffusion technique is that the wettability gradients are rather broad, ranging from millimeters to centimeters. Our group has recently demonstrated that the gradient spread can be decreased by forming the molecular gradient onto a flexible substrates made of cross-linked poly(dimethyl siloxane) (PDMS) networks that were mechanically uniaxially pre-stretched to various lengths (Δx) and uniformly exposed to ultraviolet/ozone (UVO) treatment prior to the gradient formation using the vapor diffusion technique [22]. The UVO process produced hydrophilic moieties on the surface of PDMS [23]. Efimenko and Genzer showed that the steepness and the position of the gradient on the substrate can be fine-tuned by simply choosing

the right combination of Δx, exposure time to the UVO, diffusion time, and the flux of the chlorosilane molecules in the vapor phase. Using this method planar molecular gradients ranging from several millimeters to several centimeters can be fabricated. Figure 3 shows an example of such a gradient formed on flexible substrates by depositing n-octyltrichlorosilane (OTS) molecules using the methodology described previously.

MOLECULAR GRADIENTS AS TWO-DIMENSIONAL TEMPLATES

Gradient substrates have been utilized as molecular templates for controlling the spatial distribution of non-polymeric objects. For example, Plummer and Bohn reported on electrochemically generating a gradient of amino-terminated thiol-based self-assembled monolayer on a gold-covered substrate [24]. To produce particle gradients they attached carboxylic acid-modified, fluorescently doped polystyrene nanospheres (diameter of ≈200 nm) to the amio-termini of the gradient SAM. Bhat and coworkers prepared assemblies of ≈17 nm gold colloidal nanoparticles with continuous gradients in number density on flat silica-covered substrates (Fig. 4) [25]. Their methodology consisted of: first forming a one dimensional molecular gradient of amino groups ($-NH_2$) on the substrate by vapor diffusion of amine-terminated silane molecules (aminopropyl triethoxysilane, APTES), followed by attachment of gold nanoparticles to the $-NH_2$ functional groups by immersing the substrate in a slightly acidic colloidal gold solution (pH ≈ 6.5). Under these conditions the positively charged terminus on the APTES molecules ($-NH_3^+$) is strongly attracted to the negatively charged citrate groups covering the surface of the gold nanoparticles. Experiments using scanning force microscopy revealed that the number density of nanoparticles on the substrate varied continuously as a function of the position on the substrate. NEXAFS studies confirmed that the nanoparticle number density gradient on the surface was closely correlated with the concentration gradient of $-NH_2$ groups anchored to the substrate. Bhat and coworkers demonstrated that the number density of nanoparticles within the gradient and the length of the gradient can be tuned by controlling the vapor diffusion of organosilane molecules. In addition, this simple methodology can be further extended to create double gradients, thus producing "a valley in nanoparticle concentration." The adhesive molecular template can be modified to attract different kinds of particles for different applications, all of them arranged in gradient pattern. The ability to vary and control the concentration of captured particles allows one to devise sensors, filters, etc. [6, 7].

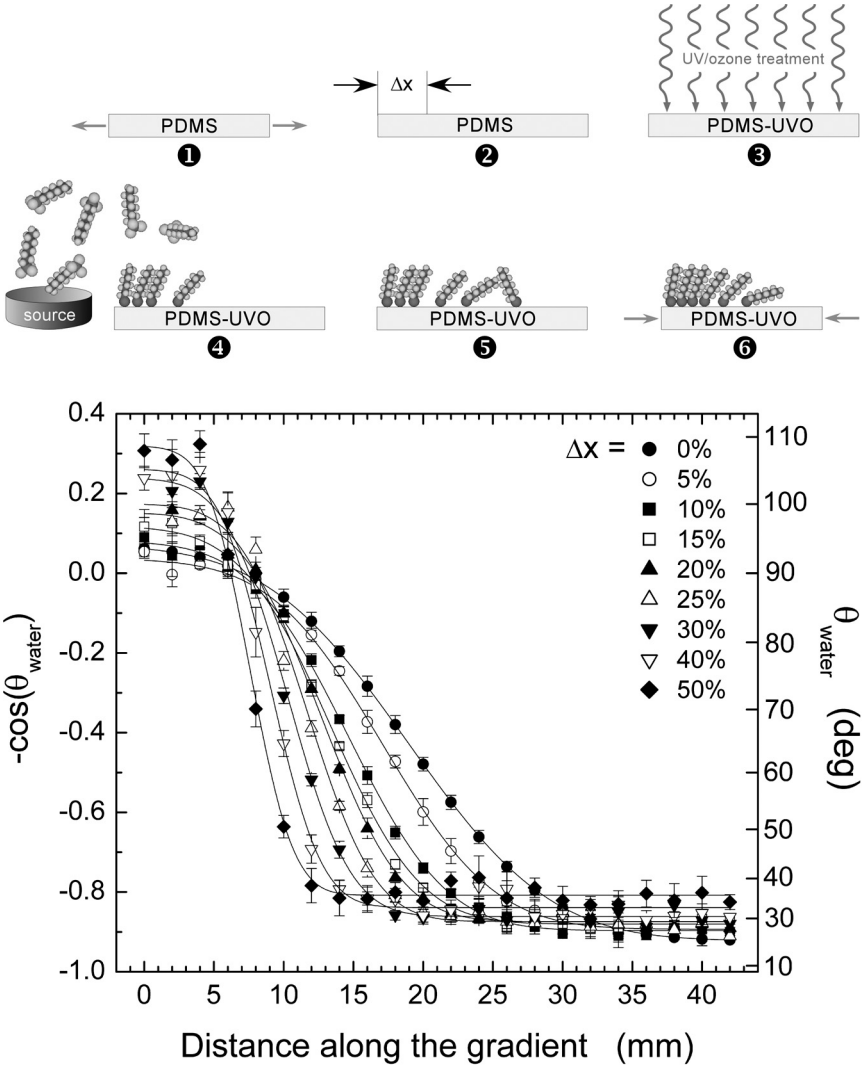

FIGURE 3 (Top panel) Schematic representation of the technological steps leading to the n-octyl trichlorosilane (OTS) molecular gradients with adjustable gradient width. See text for details. (Bottom panel) Contact angles of deionized water along OTS gradient substrates prepared on PDMS network films that were previously extended by Δx ranging from 0% to 50% [Δx equal to 0% (●); 5% (○); 10% (■); 15% (□); 20% (▲); 25% (△); 30% (▼); 40% (▽); and 50% (◆)] and treated with UVO for 30 min. The gradients were deposited from vapor (as described in the text) for 5 min. The vapor source consisted of OTS/with paraffin oil = 1:10 mixtures.

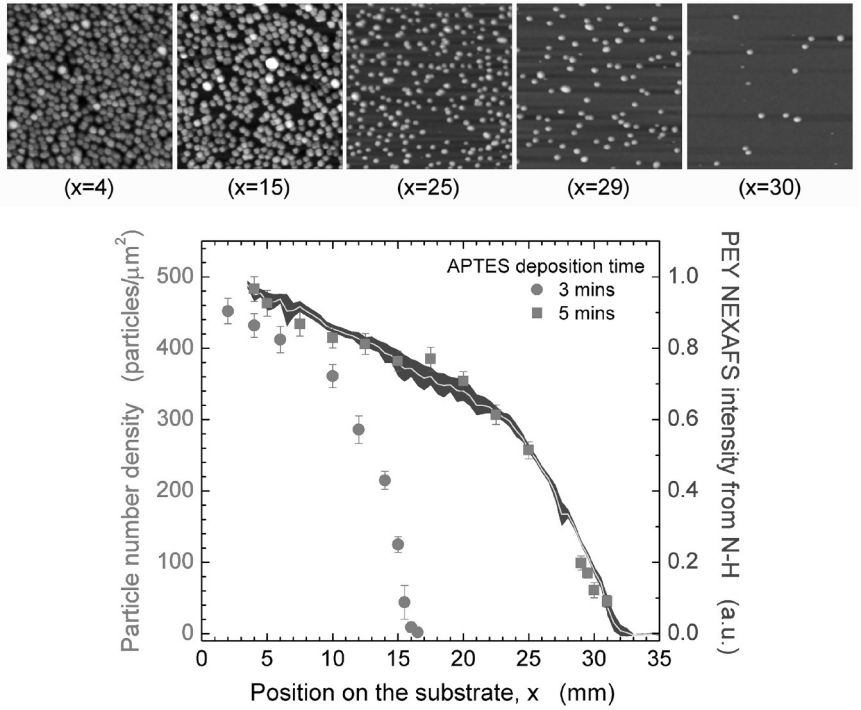

FIGURE 4 (Top panel) Scanning force microscopy images of gold nanoparticles (diameter ≈ 17 nm) adsorbed along a substrate prepared by evaporating an (3-aminopropyl) triethoxysilane (APTES)/paraffin oil (PO) mixture (50/50 w/w) for 5 min followed by immersion in colloidal gold solution (pH ≈ 6.5) for 24 hrs (Edge of each image $= 1\,\mu$m). (Bottom panel) Particle number density profile (left) for two gradients prepared by evaporating APTES/PO mixtures for 3 (●) and 5 (■) mins. The data points represent an average from 3 transverse scans along the gradient taken at the center of the sample ($y = 0$ mm) and $y = -3$ mm, and $y = +3$ mm. The line represents the partial electron yield (PEY) near-edge X-ray absorption fine structure (NEXAFS) profile (right) of N–H bonds from an ATEPS gradient prepared by evaporating APTES/PO mixture for 5 minutes. The area around the PEY NEXAFS line denotes the measurement uncertainty (based on 9 line scans along the gradient taken between -3 mm and $+3$ mm from the center of the sample). [Reprinted from reference 25, with permission from The American Chemical Society.]

ASSEMBLIES OF SURFACE-ANCHORED POLYMERS WITH GRAFTING DENSITY GRADIENTS

Molecular gradients can serve as useful templates for creating three-dimensional structures [26]. For example, Lee and coworkers utilized

the corona discharge method to produce molecular gradient of radicals on the surface of poly(ethylene). This gradient surface was then used as a template for "grafting from" radical polymerization of poly(acrylic acid) [27] and poly(ethylene oxide) [28] with gradual variation of grafting densities. Wu and coworkers recently prepared substrates with a gradient of an initiator for atom transfer radical polymerization (ATRP), on silica using the vapor diffusion technique [29, 30]. Specifically, a gradient of 1-trichlorosilyl-2-(p-chloromethylphenyl)ethane (CMPE), the polymerization initiator, was prepared on the surface using the vapor deposition technique and the unexposed regions on the substrate containing unreacted –OH functionalities were treated with OTS, in order to minimize any physisorption of monomer and/or the polymer formed in solution on the parts of the substrate that do not contain the CMPE-SAM (Fig. 5). NEXAFS was utilized to measure the concentration of the CMPE along the SAM gradient. The concentration of CMPE in the sample decreased as one moved from the CMPE side of the sample towards the OTS-SAM; the functional form closely resembled that of a diffusion-like profile. Experiments using variable angle spectroscopic ellipsometry (VASE) confirmed that only a single monolayer was formed on the substrate. Monodisperse poly(acryl amide) (PAAm) chains with gradual variation in grafting densities were synthesized by "grafting from" reaction of acryl amide using ATRP, as described earlier [31–33]. VASE was used to measure the thickness of the dry polymer film as a function of the position on the substrate. Because the polymers grafted on the substrate had all roughly the same degree of polymerization, the observed variation of the polymer film thickness was be attributed to the difference in the density, σ, of the CMPE grafting points on the substrate. The substrates with the grafted PAAm were placed into a solution cell that was filled with deionized (DI) water (pH $\approx$ 7), a good solvent for PAAm, and incubated for extended periods of time in order to allow the chains to achieve their equilibrium conformations. The wet thickness of PAAm grafted polymer in DI water, H, was measured using VASE. In Fig. 6 we plot the wet polymer thickness as a function of the PAAm grafting density on the substrate. The data in Figure 6 reveal that at low σ, H is independent of the grafting density. Hence the chains are in the mushroom regime. At high polymer grafting densities, H increases with increasing σ, indicating the brush behavior.

In addition, our group has also carried out a comprehensive study of the interfacial behavior of poly(acrylic acid) brushes with grafting density gradients as a function of the solution pH, and ionic strength. At a given pH, the brush thickness was found to be a non-monotonous function of the ionic strength. In agreement with the prediction from

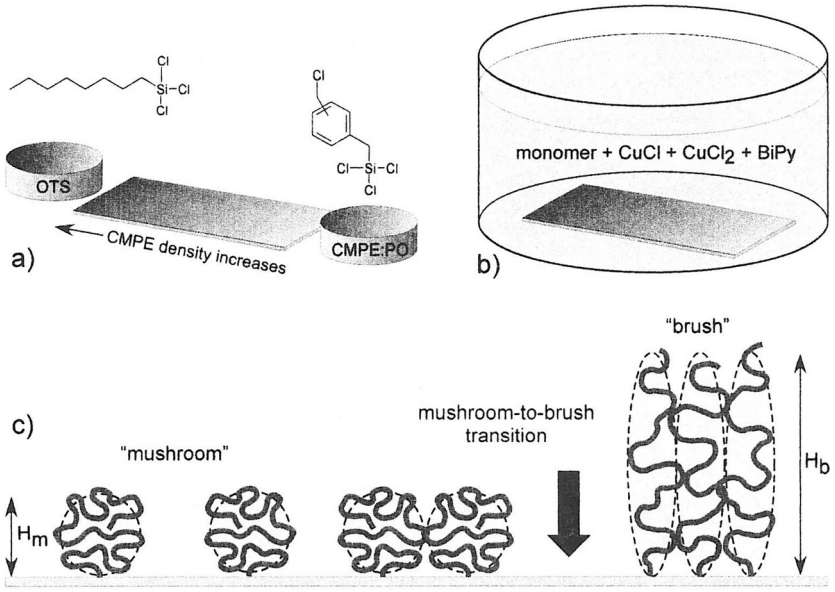

FIGURE 5 Methods of preparing surface-grafted polymer assemblies with gradients in grafting density. (a) ATRP initiator gradient on a solid substrate is formed by mixing 1-trichlorosilyl-2-(m-p-chloromethylphenyl) ethane (CMPE) with paraffin oil (PO) and placing the mixture in an open container heated at 88°C close to an edge of a silicon wafer. As CMPE evaporates, it diffuses in the vapor phase and generates a concentration gradient along the silica substrate. Upon impinging on the substrate, the CMPE molecules react with the substrate $-$OH functionalities and form a self-assembled monolayer (SAM). In order to minimize any physisorption of monomer and/or the polymer formed in solution on the parts of the substrate that do not contain the CMPE-SAM, the unexposed regions on the substrate containing unreacted $-$OH functionalities are backfilled with n-octyl trichlorosilane, (OTS). After the OTS-SAM deposition, any physisorbed CMPE and OTS molecules are removed by thoroughly washing the substrates with warm deionized water (75°C, >16 MΩ cm) for several minutes. (b) Surface-grafted polymer assemblies are formed on the substrates by using "grafting from" ATRP. (c) Schematic illustrating polymer conformations in the mushroom (height H_m) and brush (height H_b) regimes and the mushroom-to-brush transition. [Adopted from reference 26].

scaling theories of polymer brushes, we have identified three brush regimes: neutral brush, salted brush and osmotic brush. Detailed description of these experiments is outside the scope of this publication; interested reader is referred to the original source [34].

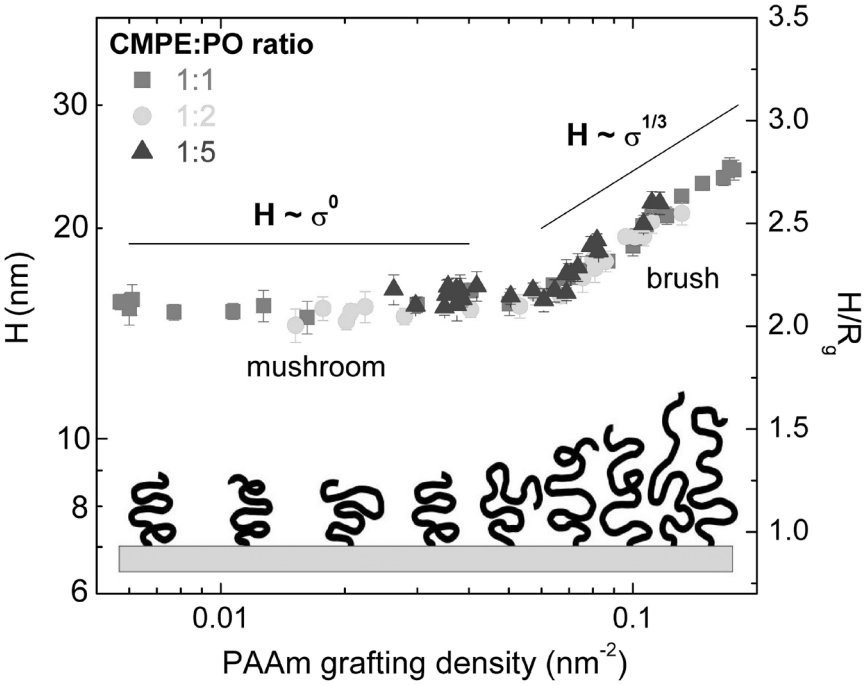

FIGURE 6 Wet thickness of PAAm as a function of the poly(acryl amide) (PAAm) grafting density for samples prepared on substrates containing the initiator gradients made of CMPE:paraffin oil mixtures (w/w) 1:1 (■), 1:2 (●), 1:5 (▲). The inset shows a cartoon illustrating the polymer behavior. [Reproduced from reference 30, with permission from The American Chemical Society.]

DIRECTED MOTION OF LIQUIDS ON GRADIENT SUBSTRATES

Chemical gradients are capable of transporting materials in a directional manner and are responsible for driving many important biological and physical processes [6]. Initial empirical observations have evolved into deliberate efforts to direct liquid motion along chemical gradients [10]. It has long been known that a continuous liquid film can spontaneously break into droplets that move freely over surfaces without application of an obvious external force. For example, the formation of wine drops from a continuous liquid film spreading over the wineglass surface ("tears of wine") is driven by the change in surface tension caused by the evaporation of alcohol. Variations in surface tension and the resulting changes in wetting behavior of the liquid

by composition or temperature gradients were studied and explained over 100 years ago and are associated with the name of the Italian physicist Carlo Marangoni [35]. As mentioned earlier, directed liquid motion due to chemical gradients on the substrate was demonstrated by Chaudhury and Whitesides [13] with droplets of water moving on a surface of varying hydrophobicity created by coating a silicon wafer partially with decyltrichlorosilane. A drop of water moved from the hydrophobic end to the hydrophilic end of the wafer, but only very slowly and only over a distance of the order of a few millimeters. Very recently much higher drop speeds have been observed for small water droplets formed by condensation of steam onto a gradient surface [36] and droplets on vibrating gradient surfaces [37].

Recently, Daniel and coworkers provided more insight about the various molecular parameters that influence the motion of liquid drops on chemically heterogeneous surfaces. They demonstrated that the drop velocity (v) is related to the surface tension of the liquid (γ), the liquid bulk viscosity (η), the radius of the droplet on the surface (R), and the position-dependent change of wettability (θ) [38]. Defining the capillary number as $\mathrm{Ca} = \mathrm{v}\eta/\gamma$, the model of Daniel and coworkers predicted:

$$\mathrm{Ca} = \mathrm{K} \cdot \mathrm{R} \frac{\partial \cos(\theta)}{\partial \mathrm{x}} = \mathrm{K} \cdot \mathrm{R}^{*}, \tag{1}$$

where the coefficient K accounts for the corrections to η due to the frictional forces at the liquid/solid interface [39], and $\mathrm{R}^{*} = \mathrm{R}\,\partial\,\cos(\theta)/\partial \mathrm{x}$ [38]. Daniel and coworkers illustrated the general validity of equation (1) by studying the motion of droplets of various liquids on surfaces covered with a molecular gradient made by depositing $H_3C(CH_2)_9Si$-SAM (H10-SAM) on flat silica-covered substrates. Data of Ca versus R^{*} from 4 different liquids had approximately identical slopes, indicating that K was very similar in all cases studied and was presumably dictated primarily by the surface energy of the substrate.

From this perspective, one can reason that higher drop velocities can be achieved by lowering the frictional forces experienced by the drop as it traverses the gradient. This concept contrasts with the earlier focus [37] on overcoming hysteresis to maximize the velocity of the drop. In order to demonstrate the above notion, we have recently prepared t-F8H2 gradients on flat silica surface and porous silica substrate and measured velocity of water droplets [40]. Combinatorial NEXAFS studies confirmed that the concentration of t-F8H2 changed gradually as a function of the position on the sample; the porous regions exhibited enhanced fluorine content relative to the non-porous part presumably because the t-F8H2 molecules also modified the walls

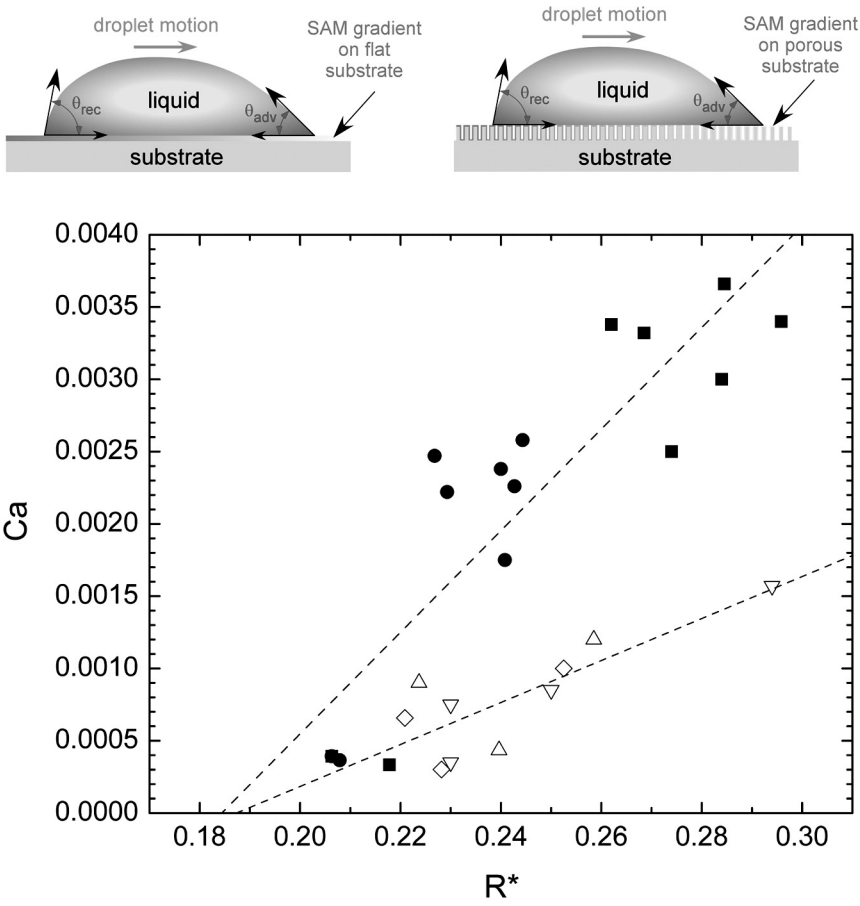

FIGURE 7 (Top panel) Schematic showing the motion of a liquid droplet on flat (left) and porous (right) surfaces. (Bottom panel) Capillary number ($Ca = v\eta/\gamma$) as a function of the normalized drop radius ($R^* = R\,\partial\cos(\theta)/\partial x$) associated with motion of a droplet of deionized water along the F8H2 molecular gradient created on top of a flat (open symbols) and porous (solid symbols) silicon substrate. During the course of the experiment the drop velocity was collected at multiple positions on the sample. The data presented have been compiled from the drop velocity data collected at the constant advancing contact angle of water equal to: 70° (▽), 65° (△), 60° (◇), 100° (■), and 80° (●). The lines are meant to guide the eye. [Reproduced from reference 40, with permission from The American Chemical Society.]

of the pores. Position-dependent contact angle measurements were used to determine the advancing and receding contact angles at various portions the substrate. The contact angle hysteresis was found to be slightly higher on the porous substrates [40]. The drop velocity was measured on various parts of the substrate for drops with several volumes (4–12 μL). The velocities determined at positions on the substrate corresponding to a constant advancing contact angle were used to evaluate Ca. Following the procedure suggested by Daniel and coworkers, the slope in Ca versus R^* plots provided a direct measure of the drop velocities (Fig. 7). Our results reveal that the velocity of water drop is approximately twice as high as the t-F8H2 substrate relative to that on the H10-SAM gradient [37]. Moreover, the graph of Ca versus R^* shows that the slope corresponding to the water droplet motion on the porous substrate is ≈2.3 times faster than the motion on the flat substrate covered with the same F8H2 molecular gradient. Our results were found to be in a good agreement with a simple scaling model that predicted the reduction of frictional forces, due to the presence of air pockets trapped inside the porous material, and the corresponding increase in the drop velocity to be about two-fold.

SUMMARY

In their work published in 1992, Chaudhury and Whitesides described a method of forming molecular gradients through vapor diffusion of organosilane precursors [13]. More than a decade later, this technique is still being used by many researchers around the world. In this paper we outlined several projects from our group that expand on the original notion of manipulating the wettability of surfaces to include the utilization of molecular gradients for controlled materials assembly and directed transportation on surfaces. In particular, molecular gradients were employed: (a) to gain better understanding of the organization of organosilane molecules in SAMs, (b) as templates for controlled deposition of nanoparticles and for the growth of surface-anchored polymer assemblies with grafting density gradient, and (c) as functional materials capable of speeding up liquid transport on porous surfaces. Recently, we have demonstrated that novel gradient materials built by exploiting vapor diffusion technique can serve as combinatorial substrates for systematic investigation of complex phenomena. For example, by combining vapor deposition technique with other materials assembly protocols, we generated orthogonal gradients in grafting density and molecular weight of surface tethered polymers [41]. These complex surface structures were used for multivariate investigation of nanoparticle adsorption on polymeric

substrates [42], for studying protein partition at surfaces [43], and tailoring cell adhesion on artificial substrates [44]. With unprecedented advances being made in the field of materials assembly, the author is hopeful that full potential of Chaudhury's simple yet powerful technique will continue to be realized in the coming years.

REFERENCES

[1] Many excellent reviews have been written on surface modification of materials. Description of methods widely used to modify surfaces of polymers can be found in: Garbassi, F., Morra, N., Occhiello, E., *Polymer Surfaces: From Physics to Technology*, (J. Wiley & Sons, New York, 1998).
[2] Ulman, A. *An Introduction to Ultrathin Organic Films from Langmuir-Blodgett to Self Assembly*, (Academic Press: New York, 1991).
[3] Chaudhury, M. K., *Mat. Sci. Eng. Rep.* **16**, 97–159 (1996).
[4] Xia, Y. and Whitesides, G. M., *Angew. Chem. Int. Ed. Engl.* **37**, 551–575 (1998); Xia, Y., Rogers, J. A., Paul, K. E., Whitesides, G. M., *Chem. Rev.* **99**, 1823–1848 (1999).
[5] For a recent review see: Edmondson, S., Osborne, V. L., and Huck, W. T. S., *Chem. Soc. Rev.* **33**, 14–22 (2004).
[6] Ruardy, T. G., Schakenraad, J. M., van der Mei, H. C., and Busscher, H. J., *Surf. Sci. Rep.* **29**, 3–30 (1997).
[7] Genzer, J. "Molecular gradients: Formation and applications in soft condensed matter science," in *Encyclopedia of Materials Science*, K. H. J. Buschow, R. W. Cahn, M. C. Flemings, B. Ilschner, E. J. Kramer, and S. Mahajan (Eds.) (Elsevier, Oxford, 2002), pp. 1–8.
[8] Genzer, J., Bhat, R. R., Wu, T., and Efimenko, K. Molecular gradient nanoassemblies, in *Encyclopedia of Nanoscience and Nanotechnology*, H. S. Nalwa, (Ed.) (American Scientific Publishers, Stevenson Ranch, CA 2004), pp. 663–676.
[9] Meredith, J. C., Karim, A., and Amis, E. J. *MRS Bull.* **27**, 330–335 (2002); Hoogenboom, R., Meir, M. A. R., and Schubert, U. S., *Macromol. Rapid Commun.* **24**, 16–32 (2003).
[10] Bain, C., *Chem. Phys. Chem.* **2**, 580–582 (2001).
[11] Carter, S. B., *Nature* **208**, 1183–1187 (1965).
[12] Elwing, H., Welin, S., Askendahl, A., Nisson, U., Lundström, I., *J. Colloid Interface Sci.* **119**, 203–210 (1987).
[13] Chaudhury M. K. and Whitesides, G. M. *Science* **256**, 1539–1541 (1992).
[14] Stöhr, J. *NEXAFS Spectroscopy* (Springer-Verlag, Berlin, 1992).
[15] Genzer, J., Fischer, D. A., and Efimenko, K., *Appl. Phys. Lett.* **82**, 266–268 (2003).
[16] The NEXAFS experiments were carried out at the NIST/Dow soft X-ray materials characterization facility at the National Synchrotron Light Source at Brookhaven National Laboratory. For detailed information about the NIST/Dow Soft X-ray Materials Characterization Facility at NSLS BNL see: http://nslsweb.nsls.bnl.gov/nsls/pubs/newsletters/96-nov.pdf.
[17] Specifically, the organosilanes were: 1H,1H,2H,2H-Perfluorodecyldimethylchlorosilane ($F_3C(CF_2)_7(CH_2)_2Si(CH_3)_2Cl$, m-F8H2), 1H,1H,2H,2H-Perfluorodecylmethyldichlorosilane ($F_3C(CF_2)_7(CH_2)_2SiCH_3Cl_2$, d-F8H2), and 1H,1H,2H,2H-Perfluorodecyltrichlorosilane ($F_3C(CF_2)_7(CH_2)_2SiCl_3$, t-F8H2).

[18] Genzer, J., Sivaniah, E., Kramer, E. J., Wang, J., Körner, H., Xiang, M., Char, K., Ober, C. K., Dekoven, B. M., Bubeck, R. A., Chaudhury, M. K., Sambasivan, S., Fishcer, D. A., *Macromolecules* **33**, 1882–1887 (2000).
[19] Banga, R. et al., *Langmuir* **11**, 4393–4399 (1995); Bunker, B. C. et al., *Langmuir* **16**, 7742–7751 (2000).
[20] Genzer, J., Fischer, D. A., and Efimenko, K., *Langmuir* **18**, 9307–9311 (2002).
[21] Genzer, J. and Efimenko, K., work in progress.
[22] Efimenko K. and Genzer, J., *Adv. Mater.* **13**, 1560–1563 (2001).
[23] Efimenko, K., Wallace, W. E., and Genzer, J., *J. Colloid Interface Sci.* **254**, 306–315 (2002).
[24] Plummer, S. T. and Bohn, P. W., *Langmuir* **18**, 4142–4149 (2002).
[25] Bhat, R. R., Fischer, D. A., and Genzer, J., *Langmuir* **18**, 5640–5643 (2002).
[26] Bhat, R. R., Tomlinson, M. R., Wu, T., and Genzer, J., *Adv. Pol. Sci.* in press (2005).
[27] Kim, H. G., Lee, J. L., Lee, H. B., and Jhon, M. S., *J. Colloid Interface Sci.* **157**, 82–87 (1993).
[28] Jeong, B. J., Lee, J. H., and Lee, H. B., *J. Colloid Interface Sci.* **178**, 757–763 (1996).
[29] Wu, T., Efimenko, K., and Genzer J. J. *Am. Chem. Soc.* **124**, 9394–9395 (2002).
[30] Wu, T., Efimenko, K., Vlček, P., Šubr, V., and Genzer J., *Macromolecules* **36**, 2448–2453 (2003).
[31] Huang, X., Doneski, L. J., and Wirth, M. J., *Chemtech* **28**, 19–25 (1998); *Anal. Chem.* **70**, 4023–4029 (1998).
[32] Huang, X. and Wirth, M. J., *Macromolecules* **32**, 1694–1696 (1999).
[33] Wu, T., Efimenko, K., and Genzer, J., *Macromolecules* **34**, 684–686 (2001).
[34] Wu, T., Genzer, J., Gong, P., Szleifer, I., Vlček, P., Subr, V., in *Polymer Brushes*, R. C. Advincula, W. J. Brittain, J. Rühe, K. Caster (Eds.) (Wiley, New York, 2004), pp. 287–316.
[35] Scriven, L. E. and Sternling, C. V. *Nature* **187**, 186–188 (1960).
[36] Daniel, S., Chaudhury, M. K., and Chen, J. C. *Science* **291**, 633–636 (2001).
[37] Daniel, S. and Chaudhury, M. K., *Langmuir* **18**, 3404–3407 (2002).
[38] Daniel, S., Sircar, S., Gliem, J., and Chaudhury, M. K., *Langmuir* **20**, 4085–4092 (2004).
[39] Greenspan, H. P. *J. Fluid Mech.* **84**, 125–143 (1978).
[40] Petrie, R. J., Bailey, T. N., Gorman, C. S., and Genzer, J., *Langmuir* **20**, 9893–9896 (2004).
[41] Bhat, R. R. Tomlinson, M. R. and Genzer J. *Macromol. Rapid Commun.* **25**, 270–274 (2004).
[42] Bhat, R. R. and Genzer J., *Appl. Surf. Sci.* in press (2005).
[43] Bhat, R. R. and Genzer, J., *Mat. Res. Soc. Symp. Proc.* **804**, JJ5.8.1–JJ5.8.9 (2004).
[44] Bhat, R. R., Chaney, B. N., Liebmann-Vinson, A., Rowley, J., and Genzer, J., submitted (2005).